

of Alkali Type on the Optical Behavior of Cu Doped Borate Glass Bandpass Filter

Ahmed Abokhadra^a, A. Samir*^b, M. A. Hassan^c, L. I. Soliman^a,
M. M. Elokr^c

^aModern Academy of Engineering and Technology, Basic Science Department, Maadi Cairo, Egypt.

^bEngineering Mathematics and Physics Department, Faculty of Engineering at Shoubra, Benha University, 11629, Egypt.

^cPhysics Department, Faculty of Science, Al- Azahr University, Cairo 11884, Egypt.

Borate oxide glass system of composition: 30Y₂O - 43B₂O₃ - 7CuO - 20ZnO where (Y= Li, Na and K) were prepared using the melt-quenching technique. Some physical properties were studied; such as X-ray diffraction, density, UV-Visible transmission spectra, ESR and FTIR. The density was measured by Archimedes method and the molar volume was calculated. It is found that density and the molar volume show opposite trend. The optical transmission was measured in the spectral range of 200–1100 nm. Some optical properties were determined. The characterized parameters of these filters, i. e. area, center, width, height and full wave at half maximum (FWHM) of band pass, have been estimated. These parameters have been found to be dependent on the alkali type. FTIR spectral studies indicate the presence of triangular and tetrahedral borate structural units. The absorption band observed in the wavelength region 550 nm in these glasses and is the characteristic of Cu²⁺ ions. ESR studies suggest that Cu²⁺ ions inter into the lattice as copper divalent state.

1. Introduction.

Nowadays, attention is being drowned to investigate oxide glasses as useful solid materials for many technological applications especially those containing transition metals. When oxide glasses doped with transition metal ions, their spectroscopic properties have been extensively studied due to variety of technological and commercial applications has been realized [1-11]. Since the incorporation of transition metal ions into glass creates colors in the glass. Recently, Cu²⁺ ion doped glasses have attracted great attention due to their peculiar optical properties [12]. In various glasses, copper can exist as Cu²⁺, Cu⁺ ions and metallic copper. A colors produced by Cu²⁺ ions have been investigated and interpreted from the view of ligand field theory [13-17]. The most important

commercial glass former is based on oxides, for example, silicate, borate, tellurite and phosphate. Borate glasses which are suitable optical materials with high transparency, low melting point, high thermal stability and good solubility making them promising candidates for a many technological applications [18-20]. It is often used as dielectric and insulating material and it is known as a good shield against infrared radiation [21,22]. The addition of alkali metal oxides, such as Na_2O , Li_2O , K_2O and Ag_2O etc. with borate backbone, reduces the melting point, improve the physical properties of these glasses as well as modify - even improve- their preparation conditions. Additionally, ZnO improves the chemical durability, melting properties, and opacity of glass, which is very important for the optical properties for glass filter [23]. The competition between the interference filters and absorption filters was increased, but the technology of fabricating the absorption bandpass filters is still very expensive and needs to have more development in chemical composition to reach the optimum practical applications [24,25].

2. Experimental Procedure

Following the conventional melt-quenching method a series of borate glasses were prepared. The prepared glass composition is $30\text{Y}_2\text{O} - 43\text{B}_2\text{O}_3 - 7\text{CuO} - 20\text{ZnO}$ where (Y= Li, Na and K). Analytical grade anhydrous powders of H_3BO_3 , ZnO , CuO and (Li_2CO_3 / Na_2CO_3 / K_2CO_3) are used as starting glass constituents. They are thoroughly mixed before placing being completely melted inside an electric furnace at 950°C for 60 min. Upon achieving the desired viscosity, the melt is then poured onto a brass mould kept at room temperature. A part of prepared samples were grinded in a gat mortar, and polished for optical measurement. X-ray diffraction (XRD) spectra were obtained on Philips Analytical X-ray diffractometer (PW3710) with Cu tube anode of wave length $K\alpha_1 = 1.5460 \text{ \AA}$ and $K\alpha_2 = 1.54439 \text{ \AA}$, to confirm the amorphous nature of the prepared samples. Data are collected at a scanning angle 2θ in the range of 10 to 70 at a rate of $0.05^\circ/\text{sec}$. Glass density is measured by Archimedes method using carbon tetrachloride as immersion liquid ($\rho = 1.592 \text{ g/cm}^3$). The ultraviolet-visible and near infrared (UV-Visb-NIR) absorption spectra in the wavelength range of 200 to 1100 nm are recorded using JENWAY 6405 UV/Vis Spectrophotometer. Infrared absorption spectra were recorded using FTIR Nicolet 6700 in the range ($2000 - 400 \text{ cm}^{-1}$). ESR measurements were carried out from 2000-5000 G range by using Bruker, EMX, ER 4119HS.

3. Result and Discussion

3.1. X-ray Diffraction

The X-ray diffraction patterns of the prepared glasses are shown in Fig. (1). The complete absence of any sharp peak indicates their amorphous nature. Moreover, the patterns exhibit a broad hump at ($2\theta \sim 30^\circ$), which is a typical feature of borate glass [26].

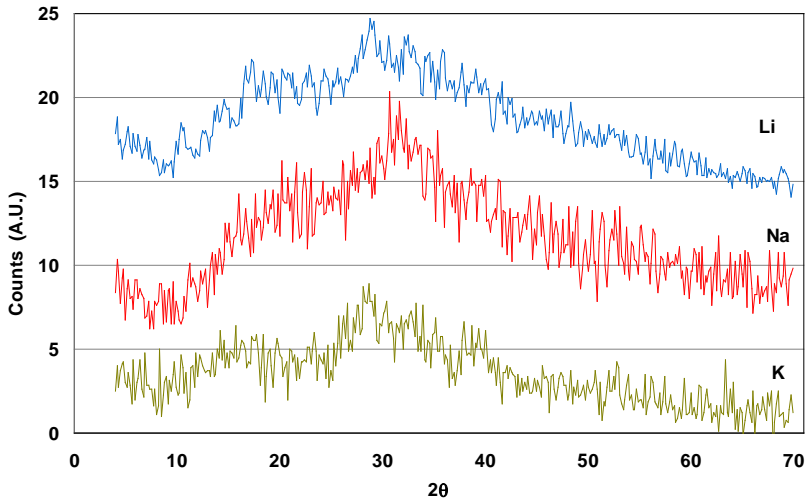


Fig. (1): The XRD patterns of the prepared samples.

3.2. Density and Molar Volume

The measured density and estimated values of the molar volume of the synthesized samples as a function of the alkali metal oxide are graphically presented in Fig. (2). In the present work the density and the molar volume show opposite behavior to each other which is the normal trend. It is found that the density decreases with change the alkali metal oxide type ($Y=Li, Na$ and K respectively) this can be attributed to the increase in the ionic radii of alkali metal oxide. Alkali metal oxides introduced into the glasses matrix act as a modifier and may not contribute to the glass formation and cleaves the structure of the glass network. Because it has a small value of the single bond strength as compared to the intermediate and glass formers.

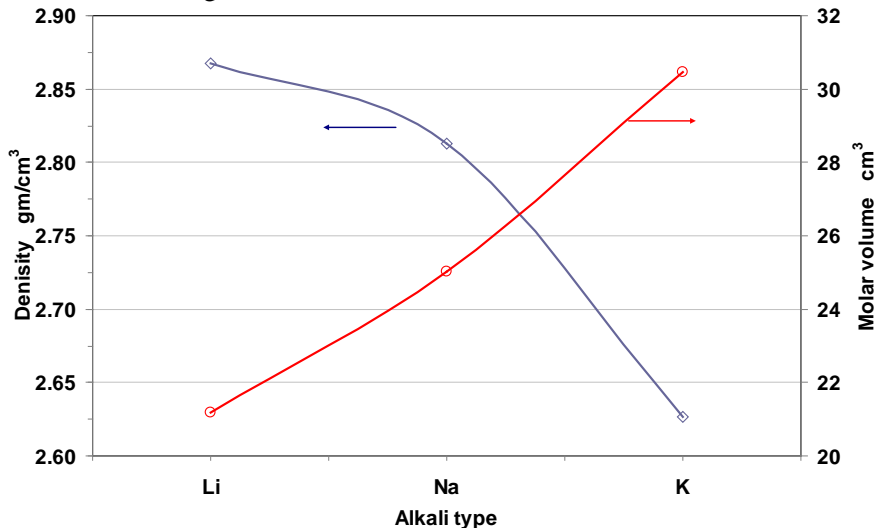


Fig. (2): Density and molar volume composition dependence.

3.3. The Optical Absorption of Glass

Figure (3) shows the UV–visible optical transmission spectra of the investigated polished glassy samples at room temperature against the wavelength 200–1100 nm. The obtained results of transmission show one asymmetric band around 485 nm, i. e. in between green and blue regions as presented in Fig. (3). The features of these bands are represented in Table (1). The bandpass filter in optics is a technique that passes a band of spectral lines through a filter. These filters have a single bandpass with double band stop in UV and IR. The dependence of cut off on UV and IR sides are listed in Table 1. Generally Filter is characterized by three parameters: central wavelength λ_{\max} , full width at half maximum (FWHM) and the area – related to the transmitted energy. The center of the peaks is located at about 482, 485, 487 nm for Li, Na and K respectively. The bands show red-shift and become narrower, the height and area decreases by replacing lithium with sodium and potassium respectively. This behavior may be attributed to the fact that; the electronegativity decreases with increasing atomic number of the alkali metal type. The spectra show a single broad absorption band in the visible- near infrared region for the prepared investigated samples as presented in Fig. (4), this can be identified as d–d transition due to copper divalent. The color of the prepared samples is green; from the complementary colors the absorbed color is red which confirm that copper has a divalent oxidation state. The corresponding ligand field parameters Dq , crystal field splitting of the energy levels of Cu^{2+} (d^9) ions in octahedral field. The absorption band corresponding to the electronic transition ${}^2E_g \rightarrow {}^2T_{2g}$ should be observed. The lack of cubic symmetry results due to the Jahn-Teller effect [12,27-29]. The crystal field strength parameter ($10Dq$) can be estimated from the band position of the copper transition, as $10Dq = \nu$ where ν is the spectral position of the absorption band [28,29]. The obtained values of the crystal field strength are tabulated in Table 1. It is clear that the $10Dq$ found to decrease as you go from Li to Na to K attributed to the lower electronegativity from Li to K, the electronegativity of the pure elements brought by using Allen scale [30].

Table (1): The cut UV, IR and the band stop and the crystal field strength ($10Dq$) for the investigated samples.

Alkali type (Y)	Band stop wavelength (nm)		Visible band characterization				Ligand field parameter
	UV	IR	Center (nm)	FWHM	Area	Height	$10Dq$
Li	200-369	610-951	482	62.5	893	11.4	1249
Na	200-394	612-927	485	56.4	595	8.4	1254
K	200-403	627-862	487	0.53	317	8.4	1277

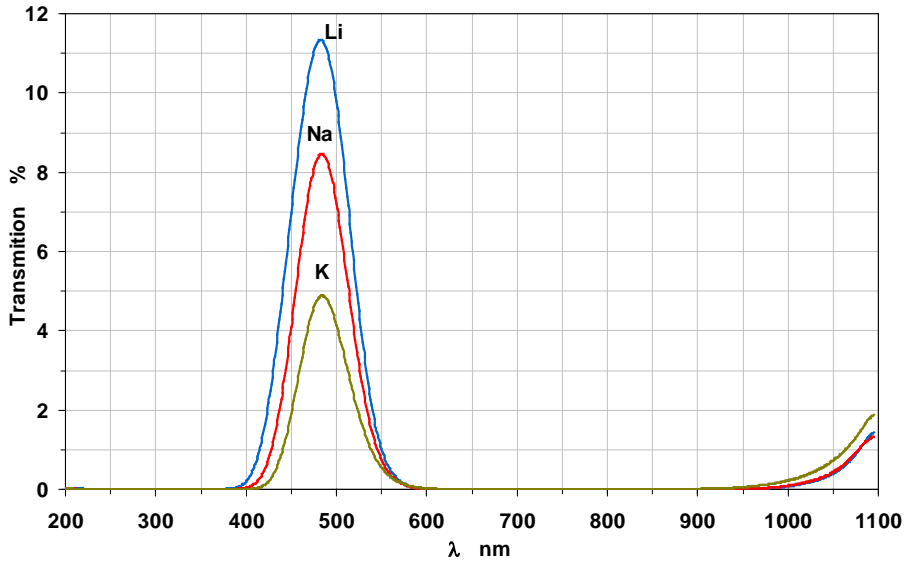


Fig. (3): Optical Transmission wavelength dependence.

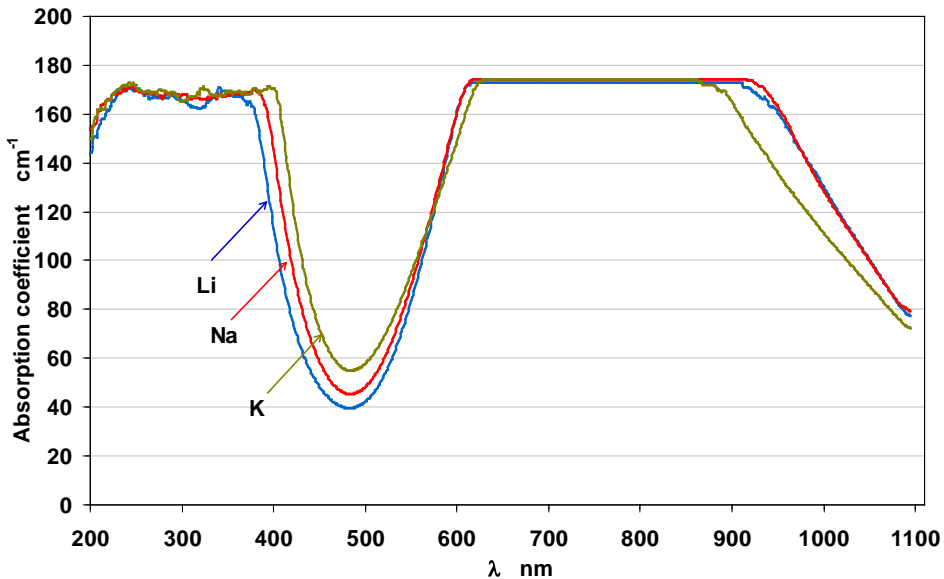


Fig. (4): Absorption coefficient as a function of the photon energy for the investigated samples.

3.4. IR Spectra

The IR spectra have been used to study the structural changes and to gain information concerning the local symmetry of the glassy systems resulting from the interactions between the boron oxide and alkali oxides atoms [11,31]. Fig. (5). Show the IR absorbance spectra for the investigated samples. All spectra consist of three main bands which are assigned to borate glasses formation. The first band

centered at $\approx 1373 \text{ cm}^{-1}$ is attributed to the asymmetric stretching vibration mode of boron triangles BO_3 . The second BO_4 band centered at $\approx 1000 \text{ cm}^{-1}$ corresponds to B–O stretching and rocking motion vibration of tetrahedral BO_4 groups. The third weak band below 700 cm^{-1} corresponds to another BO_3 groups and is attributed to deformation modes of the boron atoms perpendicular to the O_3 plans (bending vibration) of the B–O linkages in the borate network. A few overlapping bands due to different types of deformation modes are also seen. On the other hand, there exists an overlap band around $\approx 1650 \text{ cm}^{-1}$ with the triangles BO_3 band due to the O–H bending vibration mode of water. Finally a broad band around $\approx 3450 \text{ cm}^{-1}$ due to O–H vibration mode of water is also present [32-35]. The vibration of sodium and potassium ions is lay below the range of measurements in the far-infrared region [36,37].

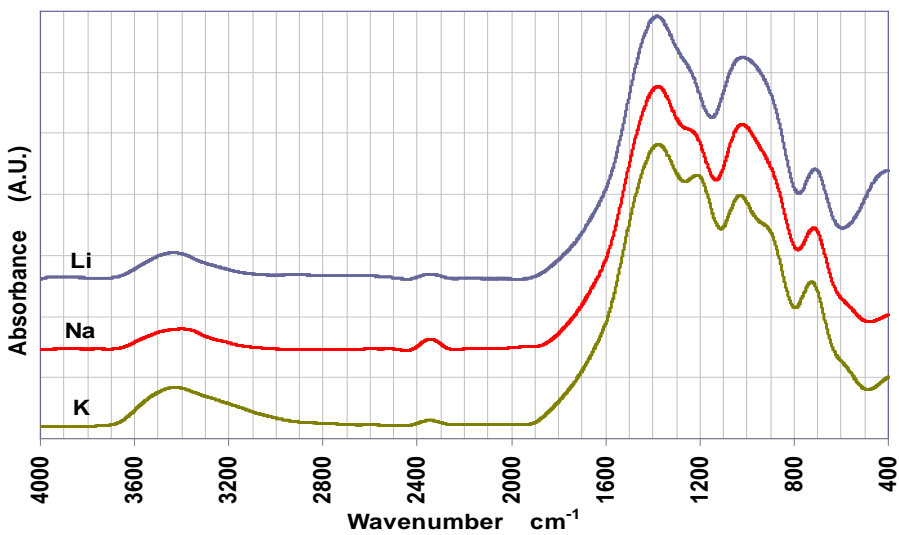


Fig. (5): FTIR spectra of alkali borate glasses doped with CuO .

3.5. ESR Measurements

Electron spin resonance (ESR) spectra of the investigated samples have been carried out at room temperature, as presented in Fig. (6). The obtained spectra show main signal band around magnetic field of order 3300 (Gauss) corresponding to presence the copper on the divalent forms [38,39]. This data are good agreement with optical data, which exhibit green color for the prepared samples. As shown in inset Fig. (6), the signals intensity is found to decrease with change alkali type from Li_2O to K_2O due to the decreasing of paramagnetic centers in the glass host [38,39].

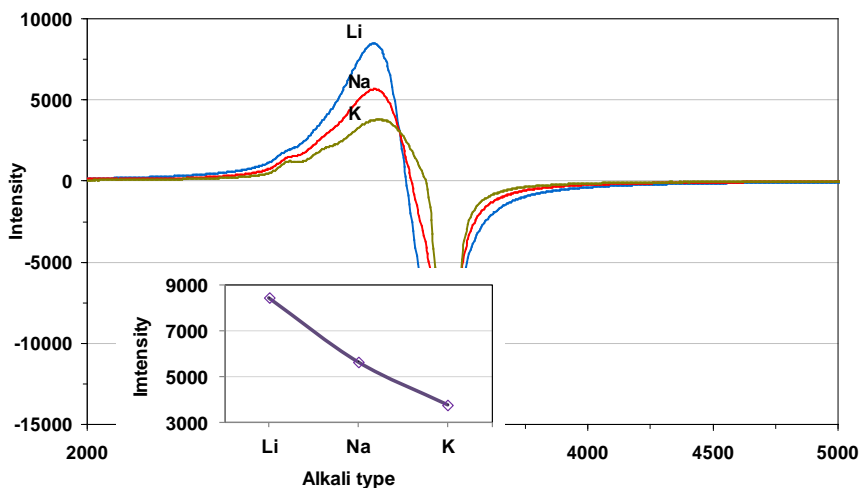


Fig. (6): ESR spectra of all the investigated glasses at room temperature, the inset figure represent the ESR intensity composition dependence.

Conclusion

The present work studies the effect of alkali oxide on the physical, structure and optical properties of the glassy system under investigation that can be used as a bandpass filter. XRD pattern confirms the amorphous nature of the investigated samples; it is observed that the density decreases with replacing the alkali oxide, while the molar volume shows opposite trend. Based on the UV–visible optical absorption studies in the present study it was found that λ_{\max} , FWHM and transmitted energy, area, is composition dependent parameter. Data obtained suggests the possibility of controlling the filtering effect. Some optical properties were studied. FTIR spectra of present glass system contains different band characteristics for BO₃, BO₄ and ZnO₄/2 structural units.

References

1. M. Subhadra, P. Kistaiah, *J. Alloys Comp.* **505**, 634 (2010).
2. H. A. ElBatal, A. M. Abdelghany, F. H. ElBatal, Kh. M. ElBadry, F. A. Moustafa, *Phys. B* **406**, 3694 (2011).
3. N. F. Mott, *J. Non-Cryst. Solids*, **1**, 1 (1968).
4. Bahra Mohammed, M.S. Jaafara, H. Wagiran, *J. Lumin.*, **190**, 228 (2017).
5. Shaweta Mohan, Kulwant Singh Thind, Gopi Sharma, Leif Gerward, *Spectrochim. Acta Part A: Mol. Biomol. Spectrosc.*, **70**, 1173 (2008).
6. M. A. F. M. da Silva, I. C. S. Carvalho, N. Cellac, H. N. Bordallo, L. P. Sosman, *Opt. Mater.*, **35** (3), 543 (2013).
7. C. R. Kesavulu, R. P. S. Chakradhar, C. K. Jayasankar, J. Lakshmana Rao, *J. Mol. Struct.*, **975**, 93 (2010).

8. W. A. Pisarski, J. Pisarska, G. Dominiak-Dzik, W. Ryba-Romanowski, *J. Alloys Comp.*, **484**, 45 (2009).
9. P. Meejitpaisan, J. Kaewkhao, P. Limsuwan, C. Kedkaew, *Proc. Eng.*, **32**, 787 (2012).
10. G. Giridhar, S. Sreehari Sastry, M. Rangacharyulu, *Phys.*, B **406**, 4027 (2011).
11. A. Terczynska-Madej, K. Cholewa-Kowalska, M. Laczka, *Opt. Mater.*, **33**, 1984 (2011).
12. Byeng-soo Bae, Michael C. Weinberg, *J. Non-Cryst. Solids*, **168**, 223 (1994).
13. A. Paul, *Chemistry of Glasses*, 2nd ed., Chapman and Hall, New York, (1990).
14. F. H. El Batal, *J. Mater. Sci.*, **43**, 1070 (2008).
15. J. Wong, C. A. Angell, *Glass Structure by Spectroscopy*, Marcel Dekker, New York, (1976).
16. H. A. ElBatal, Z. Mandouh, H. Zayed, S. Y. Marzouk, G. ElKomy, A. Hosny, *Phys.*, B **405**, 4755 (2010).
17. F. H. ElBatal, S. Y. Marzouk, N. Nada, S. M. Desouky, *Phys.*, B **391**, 88 (2007).
18. R. V. S. S. N. Ravikumar, R. Komatsua, K. Ikeda, A. V. Chandrasekhar, B. J. Reddy, Y. P. Reddy, P. S. Rao, *J. Phys. Chem. Solids*, **64**, 261 (2003).
19. U. Schoo, H. Mehrer, *Solid State Ionics*, **130**, 2436 (2000).
20. Y. M. Moustafa, A. K. Hassan, G. ElDamrawi, N. G. Yevtushenko, *J. Non-Cryst. Solids*, **194**, 34 (1996).
21. M. A. Hassan, M. Farouk, A. H. Abdullah, I. Kashef, M. M. ElOkr, *J. Alloys Comp.*, **539**, 233 (2012).
22. Min-Quan Kuang, Li-Dan Wang, Shu-Kai Duan, *J. Phys. Chem. Solids*, **111**, 41 (2017).
23. M. H. Asghar, M. Shoaib, F. Placido, S. Naseem, *Curr. Appl. Phys.*, **9**, 1046 (2009).
24. M. Bessell, *Encyclopedia of Astronomy and Astrophysics*, Nature Publishing Group and Institute of Physics Publishing, UK, (2001).
25. G. Venkateswara Rao, N. Veeraiah, *J. Alloys Comp.*, **339**, 54 (2002).
26. F. Ahmad, *J. Alloys Comp.*, **586**, 605 (2014).
27. F. A. Cotton and G. Wilkinson, *Advanced Inorganic Chemistry*, 5th Ed. (Wiley-Interscience, New York, (1988).
28. A. B. P. Lever, *Inorganic Electronic Spectroscopy*, Elsevier (1984).
29. C. A. Ballhausen, *Introduction to Ligand Field Theory*, McGraw-Hill, (1962).
30. Leland C. Allen, *J. Am. Chem. Soc.*, **111** (25), 9003 (1989).
31. J. J. Hudgens, S. W. Martin, *Phys. Rev.*, B **53** (9), 5348 (1996).
32. C. P. Varsamis, E. I. Kamitsos, G. D. Chryssikos, *Phys. Rev.*, B **60** (6), 3885 (1999).
33. S. Bhattacharya, A. Ghosh, *Chem. Phys. Lett.* **424**, 295 (2006).
34. S. Sen, A. Gosh, *J. Mater. Res.*, **15** (4), 995 (2000).
35. A. Hverhoef, H. W. Den-Hartog, *J. Non-Cryst. Solids*, 182, 221 (1995).

36. C. P. E. Varsamis, E. I. Kamitsos, *Phys. Chem. Glasses* (UK) **42** (5), 242 (2000).
37. E. I. Kamitsos, G. D. Chryssiko, *Solid State Ionics*, 109, 75 (1998).
38. Z. Y. Yao, D. Möncke, E. I. Kamitsos, P. Houizot, F. Célarié, T. Rouxel, L. Wondraczek, *J. Non-Cryst. Solids*, **435**, 55 (2016).
39. S. I. Andronenko, R. R. Andronenko, A. V. Vasil'ev, O. A. Zagrebel'nyi, *Glas. Phys. Chem.*, **30**, 230 (2004).